Thermal formation of atomic vacancies in Ni_3Al

K. Badura-Gergen and H.-E. Schaefer
Universität Stuttgart, Institut für Theoretische und Angewandte Physik, Pfaffenwaldring 57, 70569 Stuttgart, Germany
(Received 6 November 1996)

The temperature and composition dependence of the formation of thermal vacancies in the intermetallic compound Ni_3Al with the $L1_2$ structure was studied by means of positron lifetime spectroscopy. High values of the effective vacancy formation enthalpy H_V^F increasing monotonically from 1.65 ± 0.08 eV to 2.01 ± 0.08 eV with increasing Ni content from 74.1 to 76.5 at. % are found. A fit of a model based on the interaction of nearest-neighbor atoms to the experimental data demonstrates predominant formation of thermal vacancies on the Ni sublattice and high concentrations of antisite atoms. The results are discussed with respect to recent tracer-diffusion measurements in Ni_3Al. [S0163-1829(97)06530-2]

I. INTRODUCTION

Transition-metal aluminides are of interest both from the viewpoint of basic research and with respect to their potentials for technical application as high-temperature materials.[1,2] The investigation of the formation and migration of atomic defects is a prerequisite for the understanding of self-diffusion processes,[3] order-disorder phenomena,[4] creep behavior,[5] mechanical hardening,[6] or plastic deformation.[7] Positron lifetime spectroscopy is a sensitive and specific technique for studying thermal vacancy formation in pure metals[8] as well as in intermetallic phases.[9–17] For a detailed understanding of the experimental data on thermal vacancy formation in ordered intermetallic compounds a theoretical treatment of thermal defect formation in the framework of *ab initio* calculations,[7,18] embedded-atom calculations,[19,20] or empirical nearest-neighbor bond models[21–29] is necessary. A comprehensive overview of the systematics of thermal defect formation, migration, and self-diffusion in intermetallic compounds and ordered alloys was given recently.[30]

The present work aims at the investigation of the thermal vacancy formation in Ni_3Al in dependence on *temperature* and *composition* by positron lifetime spectroscopy accompanied by model calculations based on the interaction of nearest-neighbor atoms.

II. EXPERIMENTAL DETAILS

For the high-temperature positron lifetime measurements single crystals were required in order to use the technique[31] of a ^{22}NaCl positron emitter sealed into the Ni_3Al specimens. Polycrystals are unsuitable for measurements at high temperatures because of the cracking of grain boundaries[32] which gives rise to an escape of the ^{22}NaCl positron emitter. Ni_3Al single crystals of the compositions $Ni_{74.1}Al_{25.9}$ (Ref. 33) and $Ni_{76.5}Al_{23.5}$ (Ref. 34) were grown by the Bridgman technique whereas for the crystal of $Ni_{75.2}Al_{24.8}$ (Ref. 34) the zone-melting technique was applied. According to the extended phase diagram[2] of Singleton *et al.*[35] the three Ni_3Al compositions are lying within the narrow $L1_2$ phase at least up to 1550 K. The Ni content of the investigated compositions of the Ni_3Al system (see Table I) was determined by x-ray fluorescence analysis with a precision of ±0.2 at. %. Cylindrical specimens with an axial bore hole and a cover were prepared by spark erosion. After deposition of the positron emitter (about 20 μCi ^{22}NaCl) in the bore hole the specimens were sealed by electron-beam welding. In order to avoid cracking in the welding zone the two parts of the specimen were aligned crystallographically. The specimen was hermetically enclosed in a Nb container where a 2-g Cu sample was integrated in a separate chamber for performing high-precision temperature calibration at the Cu melting temperature[11] for each specimen in the temperature range where thermal vacancy formation is studied (see Fig. 1). For the high-temperature measurements the container with the specimen was electron-beam heated and the temperature was controlled by means of Pt-$Pt_{87}Rh_{13}$ thermocouples with a precision of ±5 K. The positron lifetime spectra were measured with a coincidence count rate of 70–90 cps and a total

TABLE I. Compositions of the Ni_3Al specimens together with their positron lifetime data: the free positron lifetimes τ_f at room temperature and their temperature coefficients α, the positron lifetimes in thermal vacancies τ_V as well as the vacancy formation enthalpies H_V^F, and the temperature-independent coefficients $\sigma\exp(S_V^F/k_B)$ derived from the temperature dependence of the positron trapping rate σC_V. In order to estimate the vacancy formation entropies S_V^F and the vacancy concentrations at the melting temperature $C_V(T_M)$, a specific trapping rate $\sigma=4\times10^{14}$ s^{-1} as in pure Al (see Ref. 8) was used.

	τ_f (ps)	α (10^{-5} K^{-1})	τ_V (ps)	H_V^F (eV)	$\sigma\exp(S_V^F/k_B)$ (10^{16} s^{-1})	S_V^F/k_B	$C_V(T_M)$ (10^{-4})
$Ni_{74.1}Al_{25.9}$	108 ± 1	8.6 ± 1	157 ± 3	1.65 ± 0.08	2.05 ± 2.4	3.94	4.91
$Ni_{75.2}Al_{24.8}$	110 ± 1	10 ± 1	155 ± 3	1.81 ± 0.08	5.15 ± 2.4	4.86	4.02
$Ni_{76.5}Al_{23.5}$	109 ± 1	9.7 ± 1	160 ± 3	2.01 ± 0.08	43.76 ± 24	7.0	8.42

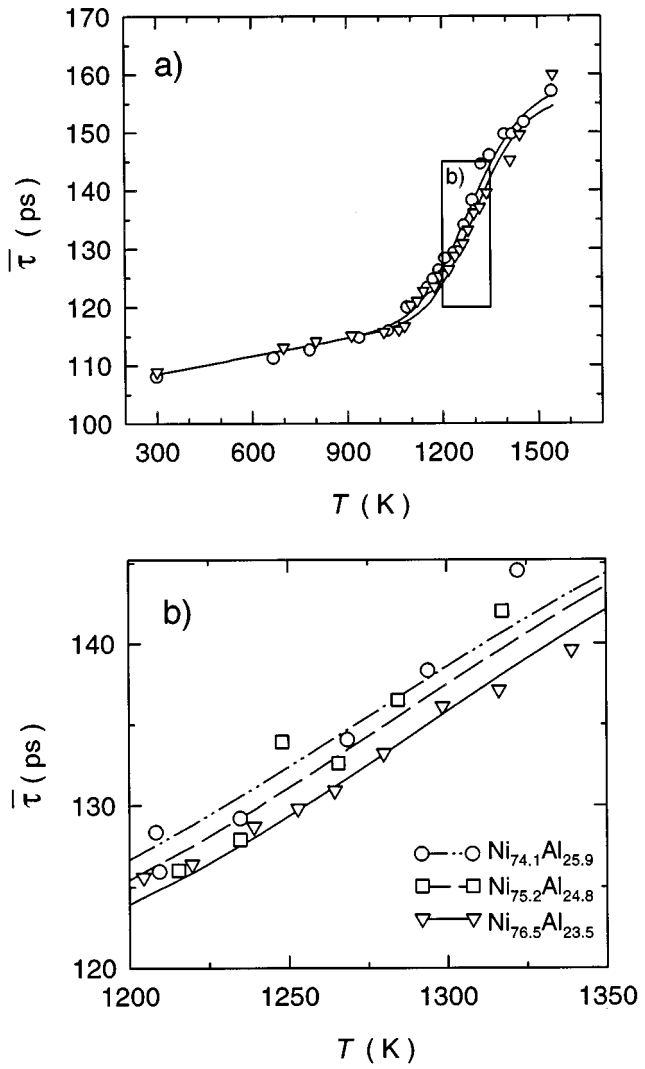

FIG. 1. Temperature dependence of the mean positron lifetime $\overline{\tau}$ in $Ni_{74.1}Al_{25.9}$ (○), $Ni_{75.2}Al_{24.8}$ (□), and $Ni_{76.5}Al_{23.5}$ (▽) together with the fit of the two-state trapping model to the experimental data.

number of 2×10^6–6×10^6 coincidence counts, making use of a fast-slow time spectrometer equipped with BaF_2 scintillators, yielding a time resolution of full width at half maximum (FWHM) of 212 ps. A numerical two-component analysis of the spectra[36] gives the time constants τ_0 and τ_V, which denote the positron residence time in the free delocalized state and the lifetime of positrons localized in vacancies, respectively, with their relative intensities I_0 and $I_V=1-I_0$.

III. EXPERIMENTAL RESULTS AND DISCUSSION

The temperature variation of the mean positron lifetime $\overline{\tau}=I_0\tau_0+I_V\tau_V$ in Ni_3Al shows for the present compositions the S-shaped behavior, which is characteristic for the annihilation of free delocalized positrons at lower temperatures and positrons annihilated with a longer lifetime at high temperatures due to trapping at thermally formed vacancies [see Fig. 1(a) and Table I].

The positron lifetime at lower temperatures was determined to $\overline{\tau}=\overline{\tau}\,(300\text{ K})\times(1+\alpha T)$ between 300 K and 1100 K with $\alpha=(9.41\pm1)\times10^{-5}\text{ K}^{-1}$.

If we compare this value of $\overline{\tau}$ at lower temperatures (Table I) and the mean valence electron density $\eta=0.731\text{Å}^{-3}$ in Ni_3Al with similar η values of pure metals and other intermetallic phases[16,33] without vacancies, these low lifetimes have to be ascribed to positrons annihilating from the free delocalized state ($\overline{\tau}=\tau_f$) without positron trapping at vacancies. From this we can conclude that no structural vacancies but antisite atoms are introduced upon deviations from the stoichiometric composition. Therefore no structural vacancies but antisite atoms are expected at deviations from the stoichiometric composition.

The strong increase of $\overline{\tau}$ between 1100 K and 1550 K [see Fig. 1(a)] is due to positron trapping and annihilation at thermal vacancies and is characterized by the appearance of an additional positron lifetime component with the time constant τ_V and the intensity I_V. Saturation trapping of positrons occurs at about 1550 K for all Ni_3Al compositions, pointing to a vacancy concentration of about 10^{-4}. Within the measuring precision the same positron lifetime $\tau_V=157\pm3$ ps in thermal vacancies is determined for all the specimen compositions (see Table I).

According to the simple two-state trapping model[37–39] the mean positron lifetime

$$\overline{\tau}=\tau_f\frac{1+\sigma C_V\tau_V}{1+\sigma C_V\tau_f} \tag{1}$$

is expressed by the positron lifetime τ_f in the free delocalized state,

$$\tau_f=\left(\frac{I_0}{\tau_0}+\frac{I_V}{\tau_V}\right)^{-1}, \tag{2}$$

by the positron lifetime τ_V in thermal vacancies and by the positron trapping rate

$$\sigma C_V=I_V\left(\frac{1}{\tau_0}-\frac{1}{\tau_V}\right) \tag{3}$$

$$=\sigma\exp\left(\frac{-H_V^F}{k_BT}\right)\exp\left(\frac{S_V^F}{k_B}\right). \tag{4}$$

Here σ denotes the specific positron trapping rate, C_V the thermal vacancy concentration, H_V^F the effective vacancy formation enthalpy, S_V^F the effective vacancy formation entropy, and k_B Boltzmann's constant.

The vacancy formation enthalpies H_V^F and the factors $\sigma\exp(S_V^F/T)$ (see Table I), which are assumed to be temperature independent, are determined from a fit of Eq. (4) to the experimental data in the temperature range between 1200 K and 1350 K.

The shift of the $\overline{\tau}$ curves is due to a monotonic increase of the vacancy formation enthalpy with increasing Ni contents.

IV. MODEL CALCULATION AND DISCUSSION

For calculating the thermal equilibrium concentration of atomic defects in Ni_3Al as a function of temperature

and composition in the framework of an empirical nearest-neighbor bond model, we make use of *Ansätze* presented earlier.[21,27,28,40,41] Here, n_{i_j} denotes the number of atoms of the type i (Ni or Al) on the sublattice j (Ni or Al), n_{V_j} the number of vacancies on the sublattice j, and $N_{Ni}=3(N-N_\delta)$ or $N_{Al}=N+3N_\delta$ the total numbers of Ni or Al atoms, respectively, where N_δ designates deviations from the stoichiometric composition and N the total number of Al atoms in the stoichiometric compound.

For the number of vacancies $n_{V_{Ni}}$, $n_{V_{Al}}$ or antisite defects $n_{Ni_{Al}}$, $n_{Al_{Ni}}$ on the Ni or Al sublattice the following equations hold:

$$n_{V_{Ni}}=N_{Ni}-n_{Ni_{Ni}}-n_{Al_{Ni}}, \tag{5}$$

$$n_{V_{Al}}=N_{Al}-n_{Al_{Al}}-n_{Ni_{Al}}, \tag{6}$$

$$n_{Ni_{Al}}=N_{Ni}-n_{Ni_{Ni}}, \tag{7}$$

$$n_{Al_{Ni}}=N_{Al}-n_{Al_{Al}}. \tag{8}$$

Here N_{Ni} or N_{Al} denote the number of lattice sites on the Ni or Al sublattice, with

$$\frac{1}{3}N_{Ni}=N_{Al}, \tag{9}$$

because of the conservation of the whole number of lattice sites. From Eqs. (5)–(8) we then obtain $N_{Ni}=3N+\frac{3}{4}(n_{V_{Ni}}+n_{V_{Al}})$. The temperature variations of the concentrations of thermal defects in thermodynamic equilibrium are derived from the configurational part of the Gibbs free enthalpy

$$G=H-TS, \tag{10}$$

where the configurational part of the enthalpy,

$$H=-\frac{4}{N_{Ni}}[(n^2_{Ni_{Ni}}+3n_{Ni_{Al}}n_{Ni_{Ni}})\epsilon_{NiNi}+(n^2_{Al_{Ni}}+3n_{Al_{Al}}n_{Al_{Ni}})\epsilon_{AlAl}+(2nNi_{Ni}n_{Al_{Ni}}+3(n_{Ni_{Ni}}n_{Al_{Al}}+n_{Ni_{Al}}n_{Al_{Ni}}))\epsilon_{NiAl}], \tag{11}$$

is represented by the sum of the probabilities of two nearest lattice sites be occupied by a certain configuration of atom pairs multiplied by the corresponding bond energies $\epsilon_{NiNi},\epsilon_{AlAl},\epsilon_{NiAl}$ between these pairs. In the formalism of Bragg and Williams[42] the ordering energy

$$\epsilon=\epsilon_{NiAl}-\frac{\epsilon_{NiNi}+\epsilon_{AlAl}}{2} \tag{12}$$

is related to the critical temperature T_c for the order-disorder transition of the alloy [Eq. (21)]. The configurational entropy of the crystal lattice,

$$S=k_B\ln\frac{N_{Ni}!}{n_{V_{Ni}}!n_{Ni_{Ni}}!n_{Al_{Ni}}!}\,\frac{N_{Al}!}{n_{V_{Al}}!n_{Al_{Al}}!n_{Ni_{Al}}!}, \tag{13}$$

is given by the total number of permutations to distribute the defect species on the sites of the two sublattices.

Equations (11) and (13) are inserted into Eq. (10) for the Gibbs free enthalpy. Minimizing G with respect to the numbers of the defect species with the aid of the Lagrange multiplier technique taking into account Eqs. (5) to (7), the following coupled nonlinear equations for the antisite-defect or vacancy concentrations in thermodynamical equilibrium are obtained (see also Refs. 21 and 28):

$$\frac{n_{Al_{Ni}}}{N_{Al}}=\frac{n_{Ni_{Al}}+3N_\delta}{N_{Al}}+\frac{3n_{V_{Al}}-n_{V_{Ni}}}{4N_{Al}}, \tag{14}$$

$$\frac{n_{Ni_{Al}}}{N_{Al}}=\frac{n_{Ni_{Ni}}n_{Al_{Al}}}{n_{Al_{Ni}}N_{Al}}\exp\left[-\frac{4}{k_BT}\left(\frac{3n_{Ni_{Al}}-n_{Ni_{Ni}}}{3N_{Al}}(\epsilon_{NiNi}-\epsilon_{NiAl})+\frac{n_{Al_{Ni}}-3n_{Al_{Al}}}{3N_{Al}}(\epsilon_{AlAl}-\epsilon_{NiAl})\right)\right], \tag{15}$$

$$\frac{n_{V_{Ni}}}{N_{Al}}=3^{3/4}\left(\frac{n_{Ni_{Ni}}}{n_{Ni_{Al}}}\right)^{1/4}\exp\left[-\frac{1}{k_BT}\left(\frac{n^2_{Al_{Ni}}+3n_{Al_{Al}}n_{Al_{Ni}}}{3N^2_{Al}}\epsilon_{AlAl}+\left(\frac{n^2_{Ni_{Ni}}+3n_{Ni\_Al}n_{Ni_{Ni}}}{3N^2_{Al}}-\frac{n_{Ni_{Ni}}-3n_{Ni_{Al}}}{3N_{Al}}\right)\epsilon_{NiNi}+\left(\frac{2n_{Ni_{Ni}}n_{Al_{Ni}}+3n_{Ni_{Ni}}n_{Al_{Al}}}{3N^2_{Al}}+\frac{3n_{Ni_{Al}}n_{Al_{Ni}}}{3N^2_{Al}}-\frac{n_{Al_{Ni}}-3n_{Al_{Al}}}{3N_{Al}}\right)\epsilon_{NiAl}\right)\right], \tag{16}$$

$$\frac{n_{V_{Al}}}{N_{Al}}=3^{3/4}\left(\frac{n_{Ni_{Al}}}{n_{Ni_{Ni}}}\right)^{3/4}\exp\left[-\frac{1}{k_BT}\left(\frac{n^2_{Al_{Ni}}+3n_{Al_{Al}}n_{Al_{Ni}}}{3N^2_{Al}}\epsilon_{AlAl}+\left(\frac{n^2_{Ni_{Ni}}+3n_{Ni\_Al}n_{Ni_{Ni}}}{3N^2_{Al}}+\frac{n_{Ni_{Ni}}-3n_{Ni_{Al}}}{N_{Al}}\right)\epsilon_{NiNi}+\left(\frac{2n_{Ni_{Ni}}n_{Al_{Ni}}+3n_{Ni_{Ni}}n_{Al_{Al}}}{3N^2_{Al}}+\frac{3n_{Ni_{Al}}n_{Al_{Ni}}}{3N^2_{Al}}+\frac{n_{Al_{Ni}}-3n_{Al_{Al}}}{N_{Al}}\right)\epsilon_{NiAl}\right)\right]. \tag{17}$$

For the determination of the model parameters $\epsilon_{AlAl}, \epsilon_{NiNi}, \epsilon_{NiAl}$ from a fit to the experimental H_V^F values the following approximations are introduced into Eqs. (14) to (17).

(i) Because the concentrations of vacancies on both sublattices are small (see Table I),

$$\frac{n_{V_{Al}}}{N}, \quad \frac{n_{V_{Ni}}}{N} \ll 1,$$

the approximation

$$N_{Al} = \frac{1}{3} N_{Ni} \approx N$$

holds. Further we assume that the concentration of thermal vacancies is smaller than those of thermal antisite atoms, which is supported by the observation that rather structural antisite atoms are formed than structural vacancies upon deviations from the stoichiometric composition. Then, for the stoichiometric composition with $N_\delta = 0$ the concentrations of antisite atoms on both sublattices are nearly equal. This is supported by calculations of the thermal concentration of antisite atoms in the framework of the above model. It furthermore appears to be plausible because of the relatively low temperature T_c of the structural order-disorder transition which occurs by the formation of antisite atoms with increasing concentrations:

$$\frac{n_{Ni_{Al}}}{N} \approx \frac{n_{Al_{Ni}}}{N}.$$

(ii) No structural vacancies can be detected with positron lifetime measurements in the nonstoichiometric compounds. Deviations from stoichiometry are therefore compensated by antisite atoms. The concentrations of antisite atoms for the Ni-rich compositions are then given by

$$\frac{n_{Ni_{Al}}}{N} \approx 3\frac{-N_\delta}{N} \quad \text{and} \quad \frac{n_{Al_{Ni}}}{N} \ll 3\frac{-N_\delta}{N}$$

and for the Ni-poor compositions by

$$\frac{n_{Al_{Ni}}}{N} \approx 3\frac{N_\delta}{N} \quad \text{and} \quad \frac{n_{Ni_{Al}}}{N} \ll 3\frac{N_\delta}{N}.$$

If the above approximations are take into account, explicit equations for the defect concentrations are obtained from Eqs. (14)–(17) for the cases of stoichiometric, Ni-poor and Ni-rich Ni_3Al.[33] The two latter cases are not valid near the stoichiometric composition. In the exponents of these equations the vacancy formation enthalpies can be identified, which depend linearly on the composition.

Some information about on which sublattice thermal vacancy formation predominantly occurs can be deduced from a fit of the approximate model equations to the vacancy formation enthalpies determined for the various compositions. If we assign the measured vacancy formation enthalpies (Table I) to the vacancy formation on the Al sublattice by using the equations for the Al-vacancy concentration, the fit yields an ordering energy $\epsilon > 0$ [Eq. (12)] which is incompatible with an ordered alloy structure with $\epsilon < 0$. This points to predominant formation of thermal vacancies on the Ni sublattice which is then described by the approximate equations for the vacancy concentration on the Ni sublattice,

$$C_{V_{Ni}} \propto \exp\left[-\frac{1}{k_B T} 2(3\epsilon + 4\epsilon_{NiNi} + 2\epsilon_{AlAl}) \right], \tag{18}$$

for the stoichiometric composition,

$$C_{V_{Ni}} \propto \exp\left[-\frac{1}{k_B T} 2\left(2\epsilon + 2\epsilon_{NiNi} + \epsilon_{AlAl} + 3\frac{N_\delta}{N}(2\epsilon - \epsilon_{NiNi} + \epsilon_{AlAl}) \right) \right], \tag{19}$$

for the Ni–rich composition, and

$$C_{V_{Ni}} \propto \exp\left[-\frac{1}{k_B T} 2\left(\epsilon + 2\epsilon_{NiNi} + \epsilon_{AlAl} + 2\frac{N_\delta}{N}(\epsilon - \epsilon_{NiNi} + \epsilon_{AlAl}) \right) \right], \tag{20}$$

for the Ni-poor composition. In the exponents of the above equations the vacancy formation enthalpies in dependence of the model parameters ϵ, ϵ_{NiNi}, and ϵ_{AlAl} can be identified and together with the experimentally determined vacancy formation enthalpies H_V^F from Table I these pair bond energies can be determined. In order to reduce the uncertainties of the datermination of the pair bond energies we have chosen the ordering energy $\epsilon = 0.092$ eV similar to the value $\epsilon = 0.09$ eV calculated according to[41]

$$\epsilon = \frac{k_B T_c}{1.64}, \tag{21}$$

with a critical temperature $T_c = 1723$ K suggested for the order-disorder transition in Ni_3Al.[43] The ϵ_{NiNi} value obtained in this way (see Table II) lies near to $\epsilon_{NiNi} = 0.3$ eV (Ref. 29) determined from the vacancy formation enthalpy for pure Ni (Ref. 8). This appears to be reasonable because both crystal structures are close packed and the nearest-neighbor distances in Ni_3Al and in pure Ni are similar.

TABLE II. Pair bond energies determined from a fit of the model equations (18)–(20) to the experimental H_V^F–values (see Table I).

ϵ (eV)	ϵ_{NiNi} (eV)	ϵ_{AlAl} (eV)
0.092	0.358	0.057

Together with these pair bond energies (Table II) Eqs. (14)–(17) were solved numerically by the iterative method or by the Newton-Raphson technique, yielding the concentrations of vacancies and antisite atoms on both sublattices.

The vacancy formation enthalpy of the Ni and Al sublattices presented in Fig. 2(a) is determined according to

$$H^F_{V_{Ni/Al}} = -k_B \frac{\partial \ln C_{V_{Ni/Al}}}{\partial (1/T)}, \tag{22}$$

within a temperature range between 300 K and 1350 K. Here $C_{V_{Ni/Al}}$ denotes the thermal vacancy concentrations on the Ni

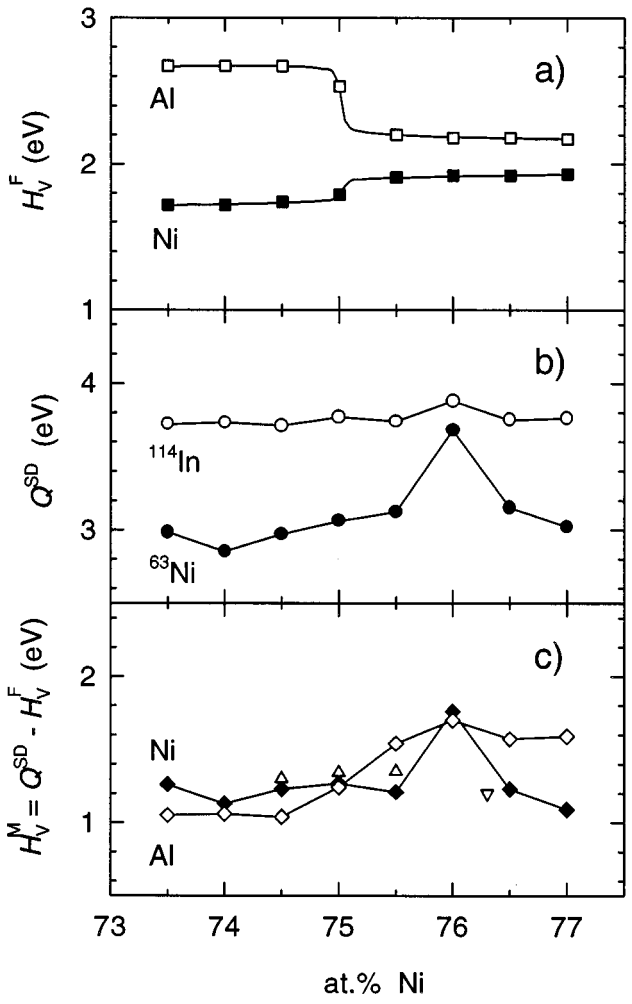

FIG. 2. (a) Calculated vacancy formation enthalpy in dependence on composition in Ni_3Al [Eq. (22)]. The nearest-neighbor bond energies ϵ_{NiNi}, ϵ_{AlAl}, and ϵ_{NiAl} presented in Table II were used. Al sublattice (□). (b) Self-diffusion enthalpy Q^{SD} determined from tracer-diffusion measurements of ^{63}Ni (●) and ^{114}In (○) as substitute for Al in Ni_3Al (Refs. 44 and 45). (c) Vacancy migration enthalpies determined according to $H_V^M = Q^{SD} - H_V^F$ for the Ni sublattice (♦) and the Al sublattice (◇) as well as activation enthalpies from recovery experiments after electron irradiation measured by means of positron annihilation (▽, Ref. 46) and of electrical resistivity (△, Ref. 47).

or Al sublattice calculated from Eqs. (16) and (17). For off-stoichiometric compositions the vacancy formation enthalpy on both sublattices depends nearly linearly on the composition. This is also seen from Eqs. (19) and (20). The change of $H^F_{V_{Ni/Al}}$ being more significant in the vicinity of the stoichiometric composition results from the relatively high critical temperature for the order-disorder transition. $H^F_{V_{Ni}}$ decreases about 0.09 eV/at. % with decreasing Ni content.[30] A similar situation is observed for Fe_3Si with decreasing Fe content.[30]

From a comparison of the calculated vacancy formation enthalpies and the self-diffusion enthalpies the vacancy migration enthalpies [Fig. 2(c)]

$$H_V^M = Q^{SD} - H_V^F \tag{23}$$

are estimated assuming simple vacancy-mediated diffusion processes as in many pure metals. The self-diffusivities Q^{SD} were determined from tracer-diffusion measurements of ^{63}Ni and ^{114}In as a substitute of Al in Ni_3Al [Fig. 2(b), Refs. 44 and 45]. The thus determined vacancy migration enthalpies are lower than the corresponding vacancy formation enthalpies and are in good agreement with experimental values determined from recovery measurements after electron irradiation by means of positron annihilation or electrical resistivity.[46,47] This points to a Ni self-diffusion process occurring via vacancies by nearest-neighbor jumps on the Ni sublattice. The higher self-diffusion enthalpies for ^{114}In than for ^{63}Ni appear to be mainly due to a lower thermal vacancy concentration on the Al sublattice than on the Ni sublattice. The maximum value of H_V^M near the stoichiometric composition [Fig. 2(c)] results from the maximum of the self-diffusion enthalpy [Fig. 2(b)] if Eq. (23) is applied. A monotonous behavior is observed for H_V^M at the stoichiometric composition. The migration enthalpies on the two sublattices are similar for the Ni-poor compositions and in the vicinity of the stoichiometric composition but differ by nearly 0.5 eV for the Ni-rich compositions. This is due to a convergence of the vacancy formation enthalpies on the two sublattices for the Ni-rich compositions [Figs. 2(a) and 2(b)]. From the present data a high ratio $H_V^F/H_V^M \geq 1$ for the formation and migration enthalpies of vacancies on the transition metal sublattice is derived for Ni_3Al similar as in pure metals. This means that the transition metal self-diffusivity is governed by low concentrations of vacancies with a high diffusivity. It furthermore means that in the concentration range $C_V \approx 10^{-5}$ of thermal vacancies detectable by positrons the equilibration times for thermal vacancies after temperature changes are in the range of milliseconds or shorter, as in pure metals.[48] In contrast to that, the ratio $H_V^F/H_V^M < 1$ is low in the transition metal aluminides with the $B2$ structure as FeAl or NiAl, according to the experimentally observed low values for vacancy formation and high values for vacancy migration enthalpies (see Ref. 30). This gives rise to a slow equilibration of thermal vacancy concentrations of about 10^{-5} which can be studied by positron lifetime spectroscopy, yielding a direct and specific determination of the vacancy migration enthalpies of $H_V^F = 1.7$ eV for FeAl (Ref. 13) and $H_V^F = 2.14$ eV for NiAl (Ref. 49).

V. SUMMARY

In conclusion the results of the present investigation on Ni_3Al may be summarized as follows.

(i) No structural vacancies are detected in the nonstoichiometric compositions. Trapping of positrons at thermal vacancies can be observed for the nearly stoichiometric composition as well as for the Ni-poor and *V*Ni-rich compositions with a positron lifetime in thermal vacancies $\tau_V = 175 \pm 3$ ps.

(ii) The two-state trapping model is applicable in the high-temperature range. The effective vacancy formation enthalpies for Ni_3Al are as high as in pure fcc metals and increase with increasing Ni content.

(iii) The comparison of the experimental data with a nearest-neighbor bond model points to a predominant vacancy formation on the Ni sublattice and yields the nearest-neighbor bond energies. From this *V*, the vacancy formation

enthalpies in a temperature range between 600 K and 1350 K on both sublattices are calculated in dependence on composition. High concentrations of thermal antisite atoms on both sublattices are derived.

(iv) The vacancy migration enthalpies on both sublattices of Ni_3Al are estimated from a comparison with the self-diffusion enthalpies of ^{63}Ni and ^{114}In (Refs. 44 and 45) and the vacancy formation enthalpies. The values are as high as in pure metals and together with the high vacancy formation enthalpies point to short vacancy equilibration times after fast temperature changes.

ACKNOWLEDGMENTS

The authors are indebted to H. P. Karnthaler and to E. Nembach for supplying Ni_3Al single crystals as well as to W. Maisch for growing Ni_3Al single crystals. Critical discussions with R. Würschum as well as the help of M. Müller in preparing the present manuscript are appreciated. The financial support by the Deutsche Forschungsgemeinschaft (Grant Nos. Scha 428/5-1, Scha 428/17-1, and Scha 428/17-2) is gratefully acknowledged. K.B.-G. appreciates financial support from the state of Baden-Württemberg during part of the present studies.

[1] J. H. Westbrook and R. L. Fleischer in *Intermetallic Compounds–Principles and Practice*, Vol 1 and 2, John Wiley, Chichester (1994).
[2] G. Sauthoff, *Intermetallics* (VCH Verlagsgesellschaft, Weinheim, 1995).
[3] H. Wever, Defect Diffusion Forum **83**, 55 (1992).
[4] E. Kentzinger, V. Pierron-Bohnes, M. C. Cadeville, M. Zemirli, H. Bouzar, M. Benakki, and M. A. Khan, Defect Diffusion Forum **143-147**, 333 (1997).
[5] G. Sauthoff, in *Diffusion in Ordered Alloys*, edited by B. Fultz, R. W. Cahn, and D. Gupta, TMS, EMPMD Monograph Series (TMS, Warrendale, 1993), p. 205.
[6] P. R. Munroe and C. H. Kong, Intermetallics **4**, 403 (1996).
[7] C. L. Fu, Y. Y. Ye, M. H. Yoo, and K. M. Ho, Phys. Rev. B **48**, 6712 (1993).
[8] H.-E. Schaefer, Phys. Status Solidi A **102**, 47 (1987).
[9] H.-E. Schaefer, R. Würschum, M. Šob, T. Žák, W. Z. Yu, W. Eckert, and F. Banhart, Phys. Rev. B **41**, 11 869 (1990).
[10] H.-E. Schaefer, R. Würschum, and J. Bub, Mater. Sci. Forum **105-110**, 439 (1992).
[11] U. Brossmann, R. Würschum, K. Badura, and H.-E. Schaefer, Phys. Rev. B **49**, 6457 (1994).
[12] K. Badura, U. Brossmann, R. Würschum, and H.-E. Schaefer, Mater. Sci. Forum **175-178**, 295 (1995).
[13] R. Würschum, C. Grupp, and H.-E. Schaefer, Phys. Rev. Lett. **75**, 97 (1995).
[14] E. A. Kümmerle, K. Badura, B. Sepiol, H. Mehrer, and H.-E. Schaefer, Phys. Rev. B **52**, 6947 (1995).
[15] R. Würschum, E. A. Kümmerle, K. Badura-Gergen, A. Seeger, Ch. Herzig, and H.-E. Schaefer, J. Appl. Phys. **80**, 724 (1996).
[16] R. Würschum, K. Badura-Gergen, E. A. Kümmerle, C. Grupp, and H.-E. Schaefer, Phys. Rev. B **54**, 849 (1996).
[17] J. Wolf, M. Franz, and T. Hehenkamp, Microchemi. Acta **125**, 263 (1997).
[18] J. Mayer, C. Elsässer, and M. Fähnle, Phys. Status Solidi B **191**, 283 (1995).
[19] S. M. Foiles and M. S. Daw, J. Mater. Res. **2**, 5 (1987).
[20] Yu. Mishin and D. Farkas, Defect Diffusion Forum **143-147**, 303 (1997).
[21] C. Y. Cheng, P. P. Wynblatt, and J. E. Dorn, Acta Metall. **15**, 1045 (1967).
[22] R. J. Wasilewski, J. Phys. Chem. Solids **29**, 39 (1968).
[23] J. P. Neumann, Y. A. Chang, and C. M. Lee, Acta Metall. **24**, 593 (1976).
[24] A. H. van Ommen, A. Waegemaekers, A. C. Moleman, H. Schlüter, and H. Bakker, Acta Metall. **29**, 123 (1981).
[25] H. Bakker and A. H. van Ommen, Acta Metall. **26**, 1047 (1987).
[26] S. M. Kim, Mater. Sci. Forum **15-18**, 1323 (1987).
[27] S. M. Kim, J. Mater. Res. **6**, 1455 (1991).
[28] S. M. Kim, Acta Metall. Mater. **40**, 2792 (1992).
[29] K. A. Badura and H.-E. Schaefer, Z. Metallkd. **84**, 405 (1993).
[30] H.-E. Schaefer and K. Badura-Gergen, Defect Diffusion Forum **143-147**, 193 (1997).
[31] K. Maier, M. Peo, B. Saile, H.-E. Schaefer, and A. Seeger, Philos. Mag. A **40**, 701 (1979).
[32] C. T. Liu, in *High-Temperature Ordered Intermetallic Alloys V*, edited by J. D. Whittenberger, I. Baker, R. Darolia, and M. H. Yoo, MRS Symposia Proceedings No. 288 (Materials Research Society, Pittsburgh, 1992), p. 3.
[33] K. Badura-Gergen, Ph.D. thesis, Universität Stuttgart, 1995.
[34] The Ni_3Al crystals with the compositions $Ni_{75.2}Al_{24.8}$ and $Ni_{76.5}Al_{23.5}$ were kindly supplied by the groups of E. Nembach and H. P. Karnthaler, respectively.
[35] M. F. Singleton, J. L. Murray, and P. Nash in *Binary Phase Diagrams*, edited by T. Massalski (ASM, Metals Park, OH, 1986), Vol. 1, p. 140.
[36] P. Kirkegaard and M. Eldrup, Comput. Phys. Commun. **7**, 401 (1974).
[37] B. Bergensen and M. J. Stott, Solid State Commun. **7**, 1203 (1969).
[38] D. L. Connors and R. W. West, Phys. Lett. **30A**, 24 (1968).
[39] A. Seeger, Appl. Phys. **4**, 183 (1974).
[40] C. Wagner and W. Schottky, Z. Phys. Chem. Abt. B **11**, 163 (1931).
[41] M. A. Krivoglaz and A. A. Smirnov, *The Theory of Order-Disorder in Alloys* (MacDonald & Co, London, 1964).
[42] W. L. Bragg and E. J. Williams, Proc. R. Soc. London, Ser. A **145**, 699 (1934).
[43] R. W. Cahn, P. A. Siemers, J. E. Geiger, and P. Bardhan, Acta Metall. **35**, 2737 (1987).
[44] Y. Shi, Ph.D. thesis, Technische Universität Berlin, 1991.
[45] Y. Shi, G. Frohberg, and H. Wever, Phys. Status Solidi A **152**, 361 (1995).
[46] T.-M. Wang, M. Shimotamai, and M. Doyama, J. Phys. F **14**, 37 (1984).
[47] B. Sitaud, C. Dimitrov, G. Dai, P. Moser, and O. Dimitrov, in *Intermetallic Compounds*, edited by O. Izumi (Japan Institute of Metals, Sendai, 1991), p. 69.
[48] H.-E. Schaefer and G. Schmid, J. Phys. Condens. Matter **1**, 49 (1989).
[49] M. Rocktäschel, Master thesis, Universität Stuttgart, 1996.